Supplemental Materials

Molecular Biology of the Cell

Topalidou et al.

Figure S1. *Eipr1* KO strategy using the CRISPR technology

(A) To make the *Eipr1* KO 832/13 cell line, Cas9-induced DNA cleavage was used toinserta puromycin cassette in the first exon of *Eipr1*. oET236, oET237 and oET200 are the primers used in (C) for detecting the positive clones.

(B) Surveyor nuclease assay testing the efficiency of three different guide RNAs (1, 2, 3) and the combination of guide RNAs #1 and #2 (1+2). All three guide RNAs recognize sequences at or around the 1st exon of rat *Eipr1*. Guide RNA #1 was used for all subsequent experiments. C: control.

(C) PCR detection of the *Eipr1* CRISPR positive clones using the indicated primers. Primers oET236 and oET237 detect clones positive for the puromycin insertion. Primers oET236 and oET200 detect clones that contain the wild type product. Clones #3 and #5 were selected as candidate *Eipr1* KOs. AWestern blot showed that clone #3 lacked EIPR1 expression (Figure 1A), but that #5 still expressed the wild type EIPR1 product. Clone #3 was used for all the *Eipr1* KO experiments in this study.

Figure S2. EIPR1 knock out does not affect transcription of DCV cargos and EARP or GARP subunits.

No change in transcript abundance of (A) proinsulin and PC1/3 or (B) VPS50 and VPS51 in *Eipr1* KO cells as measured by qRT-PCR. Actin served as an internal control. The Cq mean for the target genes was normalized against the Cq mean for the actin control.

Figure S3. *Eipr1* knock out cells have exocytosis defects.

WT and *Eipr1*KO 832/13 cells stably expressing NPY-pHluorin were imaged using spinning-disk confocal microscopy. Cells were reset for 2hrs in low K+ Krebs-Ringer buffer with 1.5mM glucose. Cells were then imaged in low K+ Krebs-Ringer buffer with

1.5mM glucose for 15 s, and stimulated with 60mM K+ and 16.7mM glucose for 80s. Images (100ms exposure) were collected at 10 Hz. Exocytotic events were hand-counted. Bar graphs show the number of exocytotic events per second normalized to cell surface area. ***, $p<0.001$, *$p<0.05$, ns $p>0.05$, error bars = SEM. Three experiments were performed on different days and plotted separately. The *Eipr1* KO showed reduced stimulated exocytosis on days 1 and 2, but no significant difference from WT on day 3. However, very few events were observed on day 3, even for WT (note the scale of the y-axis), suggesting problems on that day with the stimulation protocol or ability to detect events. On day 1, n=47 cells for WT (four coverslips imaged separately with 20, 12, 7, and 8 cells); n=43 cells for *Eipr1* KO (three coverslips with 17, 14, and 12 cells). On day 2, n=79 cells for WT (four coverslips with 26, 13, 22, and 18 cells); n=61 cells for *Eipr1* KO (three coverslips with 29, 24, and 8 cells). On day 3, n=30 cells for WT (two coverslips with 12 and 18 cells); n=11 cells for *Eipr1* KO (two coverslips with 8 and 3 cells).

Figure S4. The pH of the Golgi is not significantly changed in *Eipr1* KO cells.

(A) Example calibration curve for Golgi pH measurements based on measuring the fluorescence of TGN-targeted pHluorin in solutions of defined pH. For each biological replicate of WT and *Eipr1* KO 832/13 cells tested for pH, an individual calibration curve such as the one shown was obtained from WT and *Eipr1* KO cells grown in the same 96-well plate as the test samples and exposed to buffers of decreasing pH (8.5–5.5) in the presence of nigericin and monensin (see Materials and Methods). Each data point shows the mean of the fluorescent measurements (in arbitrary units (AU)) from cells in three different wells. Error bars=SEM.

(B) The late-Golgi compartment is not more acidic in *Eipr1* KO 832/13 cells. The fluorescence of TGN-targeted pHluorin was measured in WT and *Eipr1*KO cells. The

absolute pH value of each sample was extrapolated from a paired calibration curve (as in A). The data show mean ± SEM; n=8 for WT and *Eipr1*KO.The data shown for the WT are the same shown in Figure S3 of (Cattin-Ortolá, Topalidou*et al.*, 2019) since these experiments were run in parallel with the same WT control.

Figure S5. Mature CPE is localized in insulin-containing DCVs.

Representative images of 832/13 (WT) cells costained with antibodies for mature CPE (CPE-C) and insulin. Scale bars: 5 µm.

Figure S6.Expression of constitutively active RAB-5(QL)in neuronal cells partially rescues the NLP-21::Venus defect of *eipr-1 C. elegans*mutants

(A) Representative images of NLP-21::Venus fluorescence in motor neuron axons of wild type (WT), *rab-2(nu415),* and *eipr-1(tm4790)* mutant strains, with or without RAB-5(QL). Scale bar: 10 µm.

(B) Quantification of NLP-21::Venus fluorescence levels in motor neuron axons of the indicated strains. The mean fluorescence intensity is given in arbitrary units. *rab-2(nu415)* and *eipr-1(tm4790)* mutants have decreased levels of NLP-21::Venus fluorescence. This phenotype is partially rescued by expressing RAB-5(QL). (n = 10-20,error bars = SEM, * $p<0.05$, ** $p<0.01$, *** $p<0.001$).

(C) Representative images of of 832/13 (WT) and *Eipr1* KO cells transfected with GFP::RAB5A(QL) and costained with antibodies for GFP and mature CPE (CPE-C). Scale bars: 5 µm.

(D) *Eipr1* KOcells have an increased Golgi/cytoplasmic ratio of mature CPE relative to wild type cells and this phenotype is not rescued by expression of GFP::RAB5A(QL). Fluorescence of a region of interest that includes the TGN divided by the fluorescence of

a region of the same size in the cytoplasm, in WT and *Eipr1* KO with or without GFP::RAB5A(QL). (n=11-16, error bars = SEM, ns p>0.05)

Figure S7. Localization of VPS51::Myc and VPS53::Myc is disrupted in *Eipr1* KO cells, but VPS54::GFP is not affected

(A) Representative images of 832/13 (WT) and *Eipr1* KO 832/13 (Eipr1KO) cells transfected with VPS51::13Myc (VPS51::Myc) and stained with anti-Myc antibody. VPS51::Myc is punctate in WT cells, but diffuse throughout the cytoplasmin *Eipr1* KO cells. Scale bars: 5 μm.

(B) Representative images of 832/13 (WT) and *Eipr1* KO 832/13 (Eipr1KO) cells transfected with VPS53::13Myc (VPS53::Myc) and stained with anti-Myc antibody. VPS53::Myc is punctate in WT cells, but diffuse throughout the cytoplasm in *Eipr1* KO cells. Scale bars: 5 μm.

(C) Representative images of 832/13 (WT) and *Eipr1* KO 832/13 (Eipr1KO) cells transfected with VPS54::GFP (VPS54::GFP) and stained with anti-GFP and TGN38 antibodies. In both WT and *Eipr1* KO cells, VPS54::GFP is localized to perinuclear puncta that largely overlap with TGN38. Scale bars: 5 μm.

Figure S8. TGN38 is redistributed in *Vps51* knockdown but not *Eipr1* KO cells

Representative images of 832/13 cells (WT),*Vps51*siRNA knockdown 832/13 cells (Vps51KD), and *Eipr1* KO cells (Eipr1KO) stained for TGN38. TGN38 is partially redistributed to cytoplasmic puncta in VPS51 knockdown cells, but is still localized to the Golgi in *Eipr1* KO cells.

Figure S9. The EARP-specific component VPS50 localizes to two distinct compartments

(A) VPS50 but not CCDC186 partially colocalizes with transferrin. (Left) Representative confocal images of 832/13 cells incubated with Alexa 568-labeled transferrin (Tf) and immunostained for either VPS50 (upper) or CCDC186 (lower). Scale bars: 5 μm. (Right) Pearson's correlation coefficient was measured to quantify the localization between transferrin and CCDC186 (n=17) or transferrin and VPS50 (n=25).*** $p<0.001$, error bars = SEM.

(B) CCDC186 localization is not altered in *Eipr1* KO cells. Representative confocal images of WT and *Eipr1* KO 832/13 cells immunostained for TGN38 and CCDC186. Scale bars: 5μm.

(C,D) VPS50 only weaklycolocalizes with immature and mature DCV markers. Representative confocal images of 832/13 cells immunostained for VPS50 together with syntaxin 6 (iDCVs) or insulin (mature DCVs). Scale bars: 5 μm.

(E) VPS50 only weakly colocalizes with proinsulin, but VPS54::Myc largelycolocalizes with proinsulin at or near the TGN. Representative confocal images of 832/13 cells or 832/13 cells transiently transfected with VPS54::13Myc and immunostained for VPS50 or Myc and proinsulin. Scale bars: 5 μm.

Figure S1

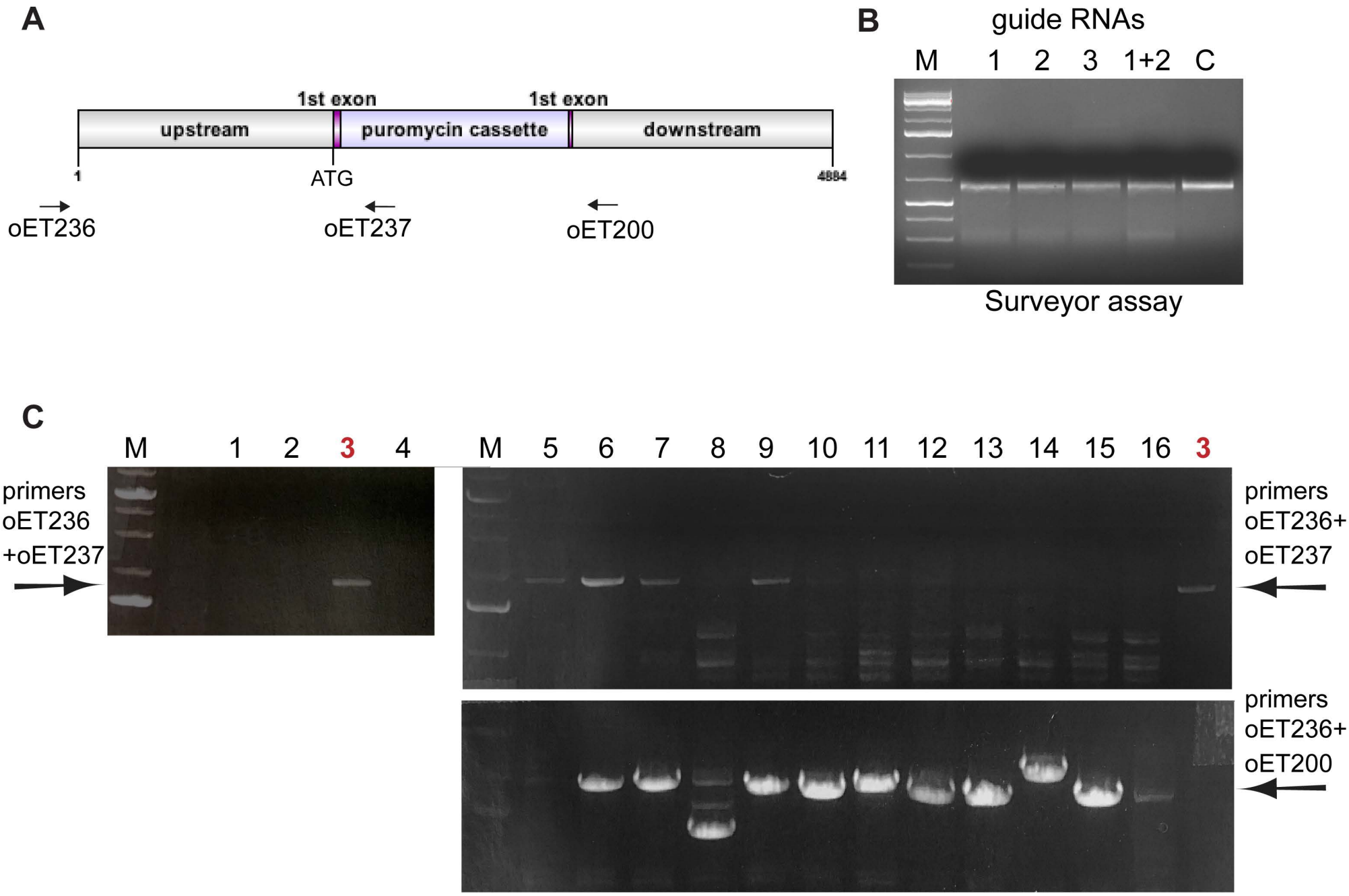
A
1st exon
1st exon
upstream
puromycin cassette
downstream
1
ATG
4884
oET236
oET237
oET200
B
guide RNAs
M
1
2
3
1+2
C
Surveyor assay
C
M
1
2
3
4
M
5
6
7
8
9
10
11
12
13
14
15
16
3
primers
oET236
+oET237
primers
oET236+
oET237
primers
oET236+
oET200

Figure S2

A

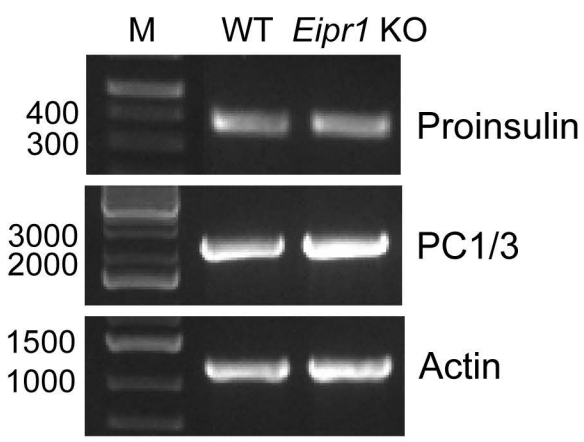
M
WT
Eipr1 KO
400
300
Proinsulin
3000
2000
PC1/3
1500
1000
Actin

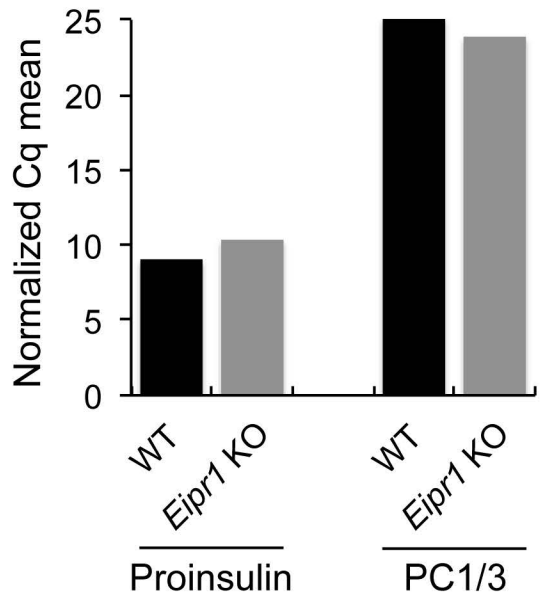
Normalized Cq mean
25
20
15
10
5
0
WT
Eipr1 KO
WT
Eipr1 KO
Proinsulin
PC1/3

B

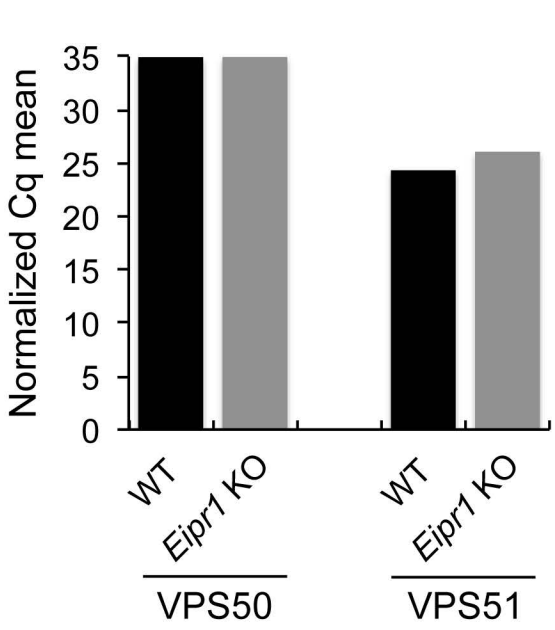
Normalized Cq mean
35
30
25
20
15
10
5
0
WT
Eipr1 KO
WT
Eipr1 KO
VPS50
VPS51

Figure S3

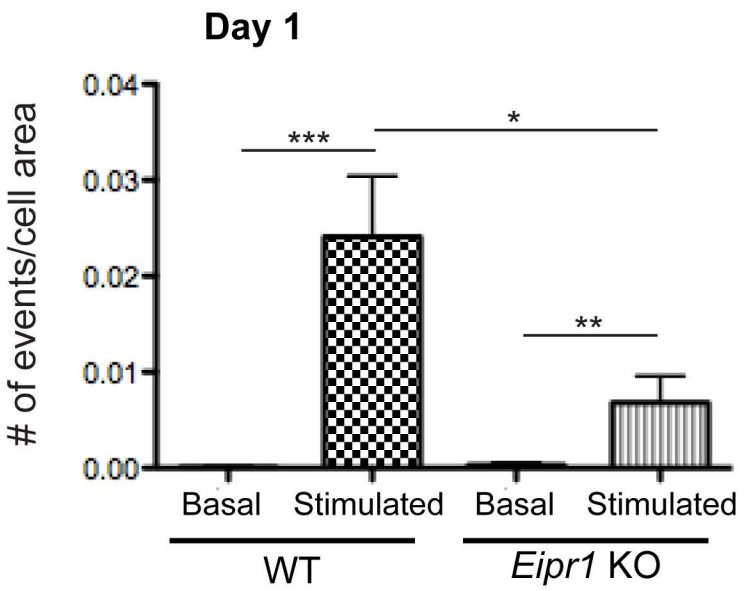
Day 1
# of events/cell area
0.04
0.03
0.02
0.01
0.00
***
*
**
Basal
Stimulated
Basal
Stimulated
WT
Eipr1 KO

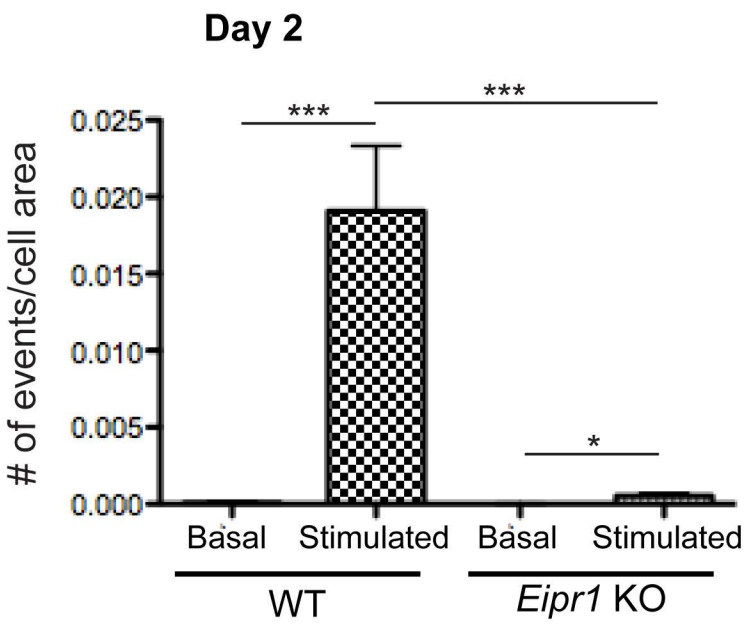
Day 2
# of events/cell area
0.025
0.020
0.015
0.010
0.005
0.000
***
***
*
Basal
Stimulated
Basal
Stimulated
WT
Eipr1 KO

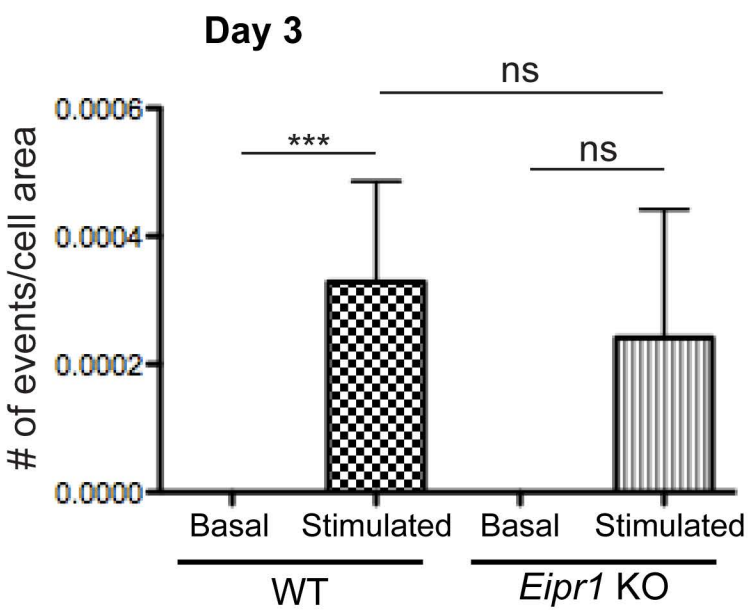
Day 3
# of events/cell area
0.0006
0.0004
0.0002
0.0000
ns
***
ns
Basal
Stimulated
Basal
Stimulated
WT
Eipr1 KO

Figure S4

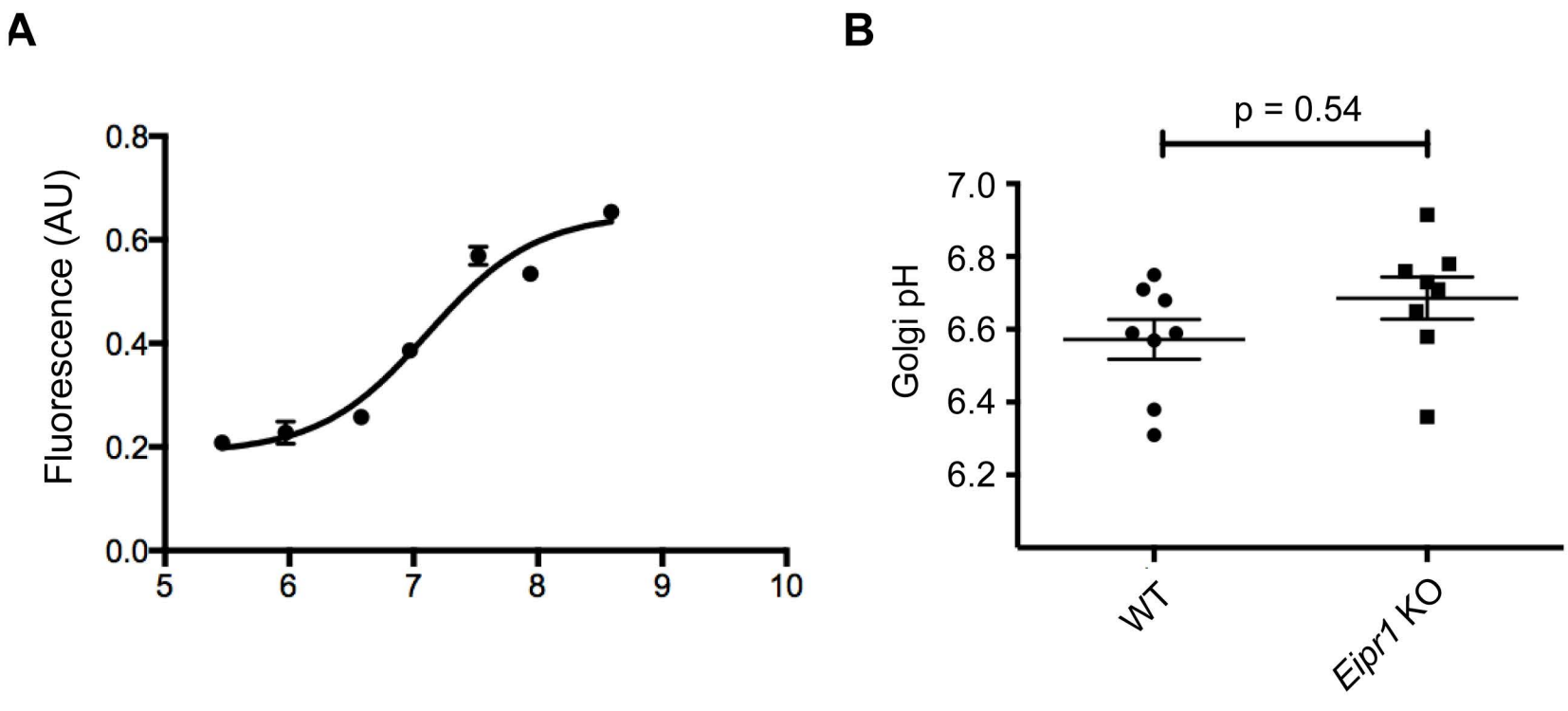
A
Fluorescence (AU)
0.0
0.2
0.4
0.6
0.8
5
6
7
8
9
10
B
p = 0.54
Golgi pH
6.2
6.4
6.6
6.8
7.0
WT
Eipr1 KO

Figure S5

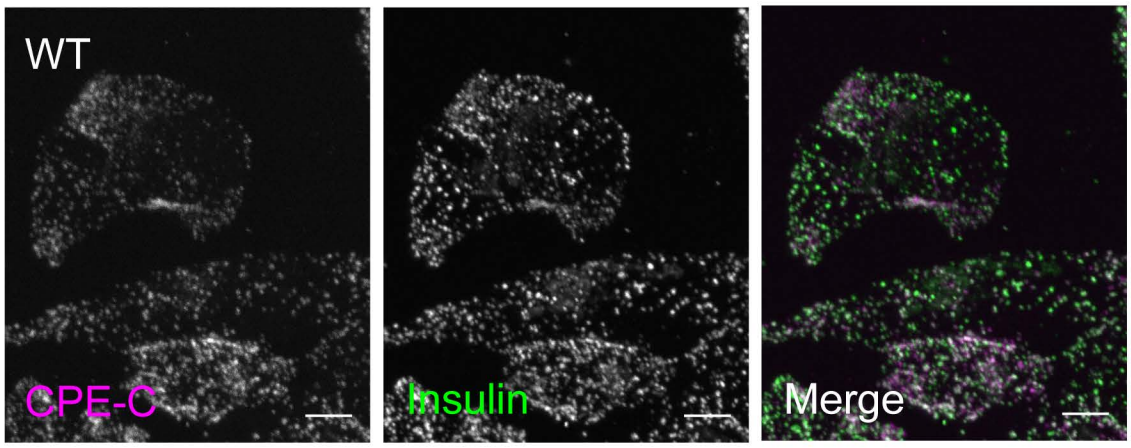

Figure S6

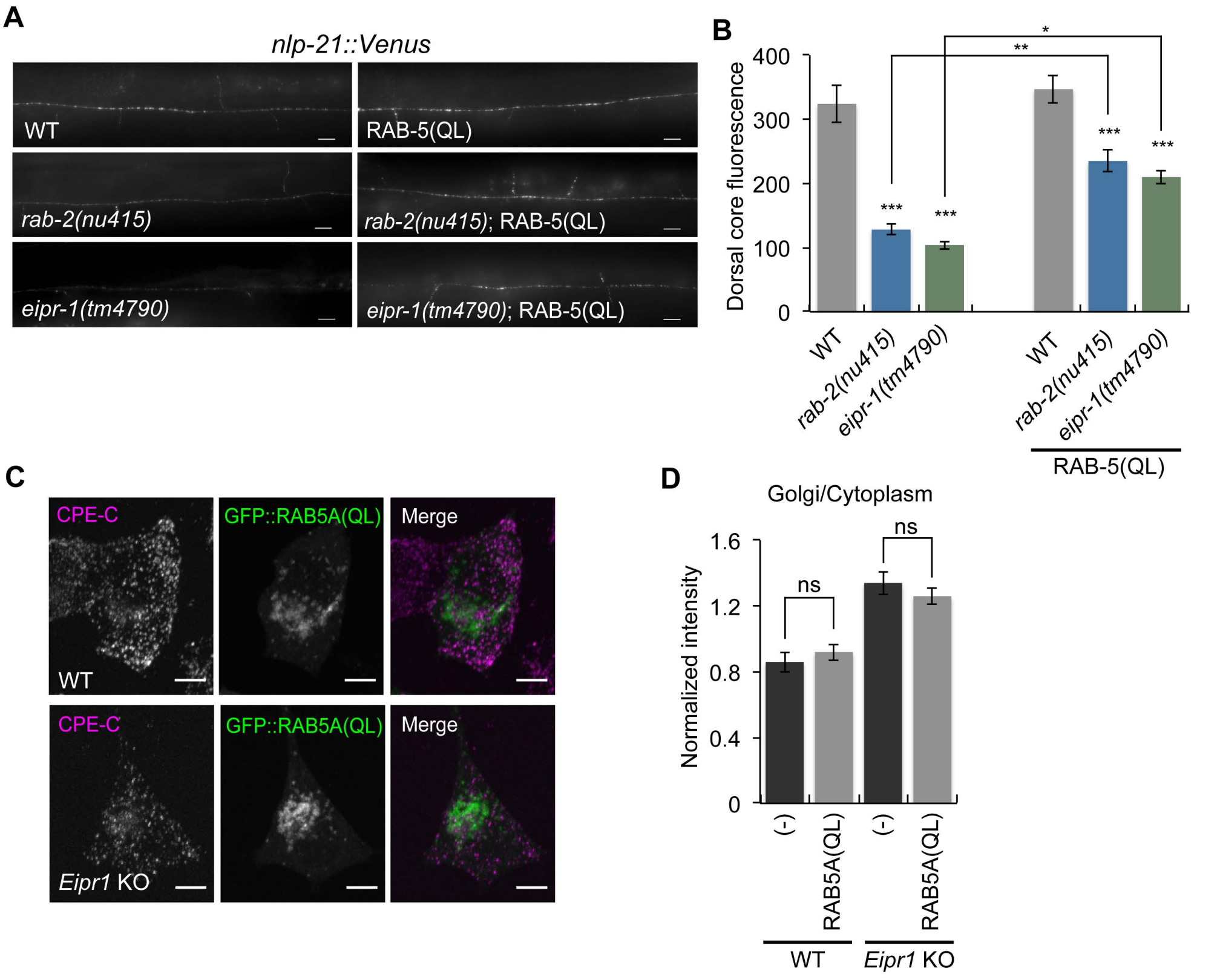
A
nlp-21::Venus
WT
RAB-5(QL)
rab-2(nu415)
rab-2(nu415); RAB-5(QL)
eipr-1(tm4790)
eipr-1(tm4790); RAB-5(QL)
B
Dorsal core fluorescence
400
300
200
100
0
*
**
***
***
***
WT
rab-2(nu415)
eipr-1(tm4790)
WT
rab-2(nu415)
eipr-1(tm4790)
RAB-5(QL)
C
CPE-C
GFP::RAB5A(QL)
Merge
WT
CPE-C
GFP::RAB5A(QL)
Merge
Eipr1 KO
D
Golgi/Cytoplasm
Normalized intensity
1.6
1.2
0.8
0.4
0
ns
ns
(-)
RAB5A(QL)
(-)
RAB5A(QL)
WT
Eipr1 KO

Figure S7

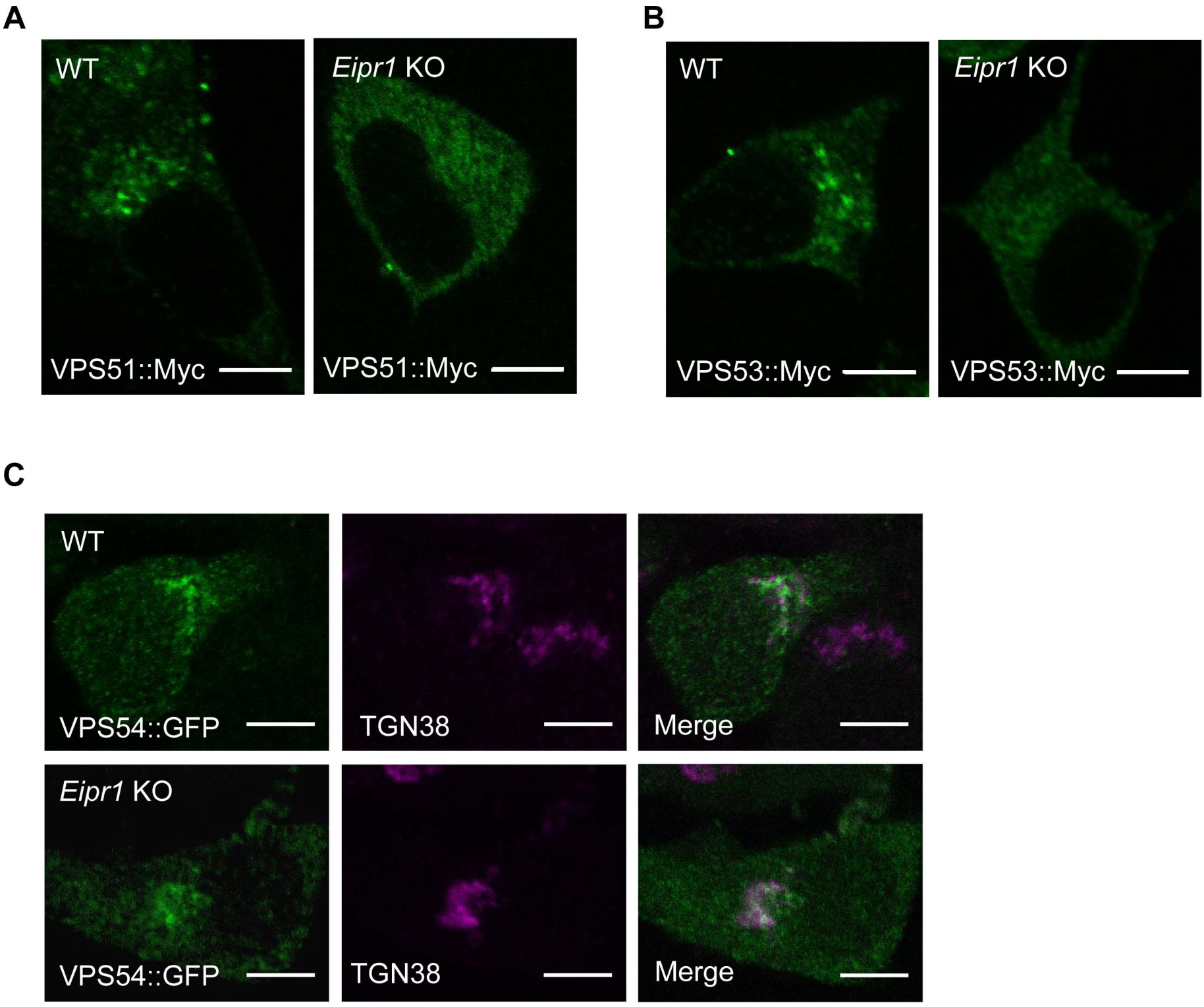
A
WT
VPS51::Myc
Eipr1 KO
VPS51::Myc
B
WT
VPS53::Myc
Eipr1 KO
VPS53::Myc
C
WT
VPS54::GFP
TGN38
Merge
Eipr1 KO
VPS54::GFP
TGN38
Merge

Figure S8

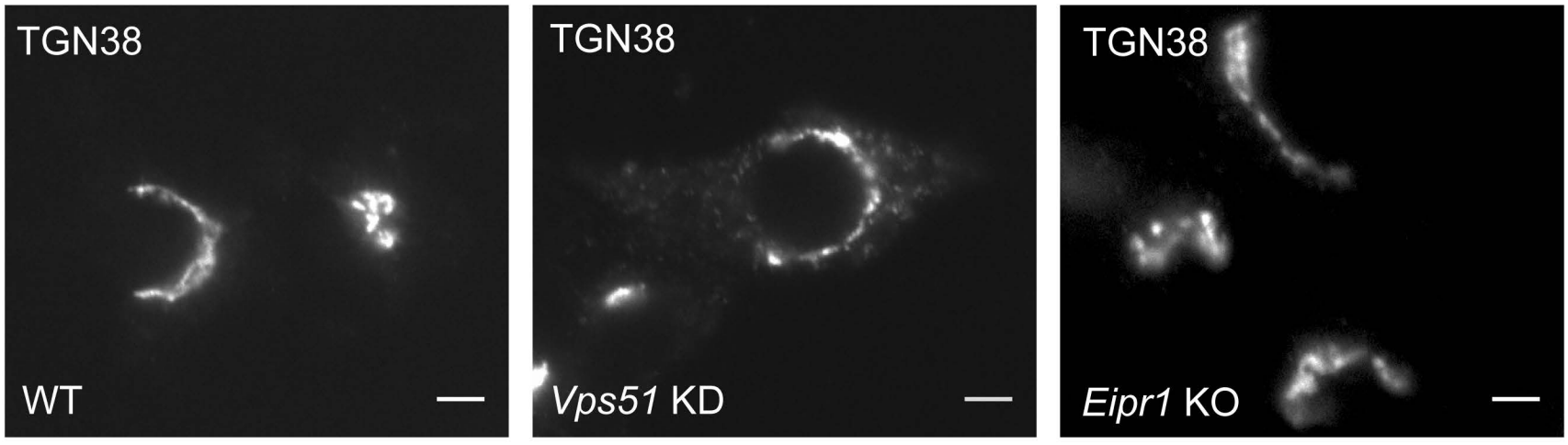

Figure S9

A

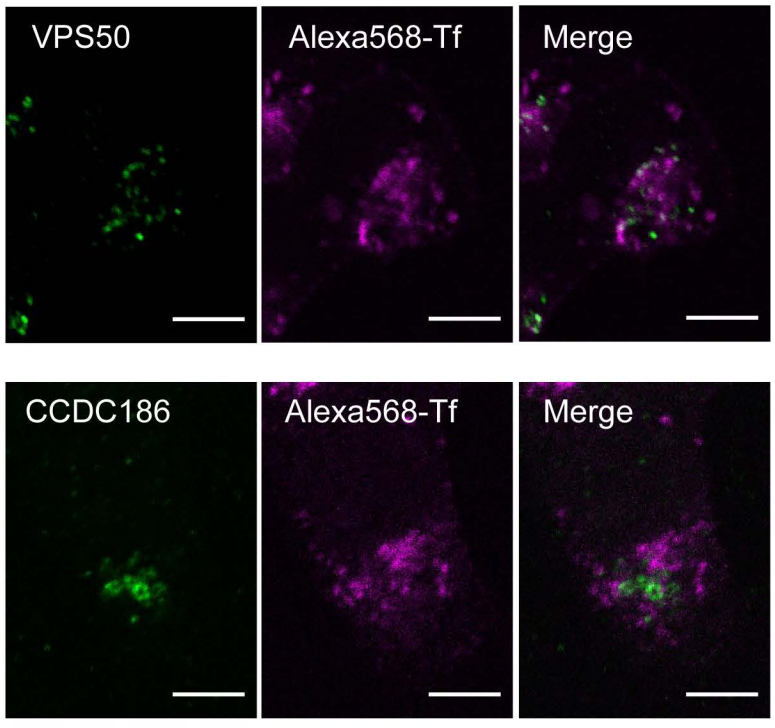

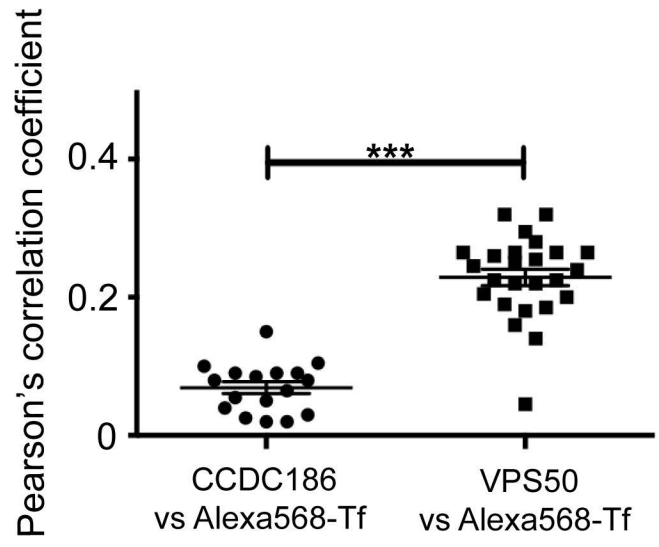

B

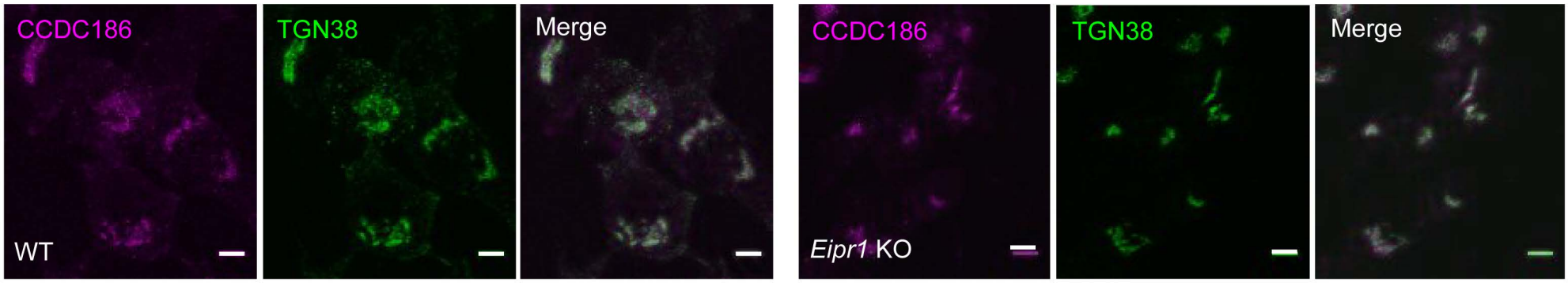

C

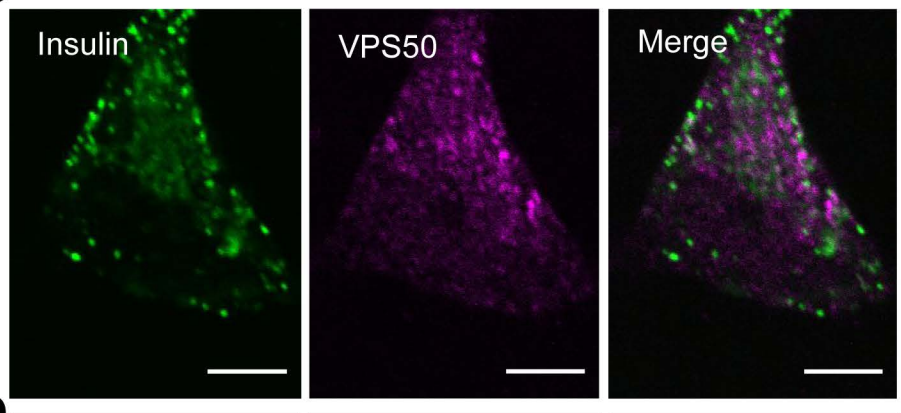

D

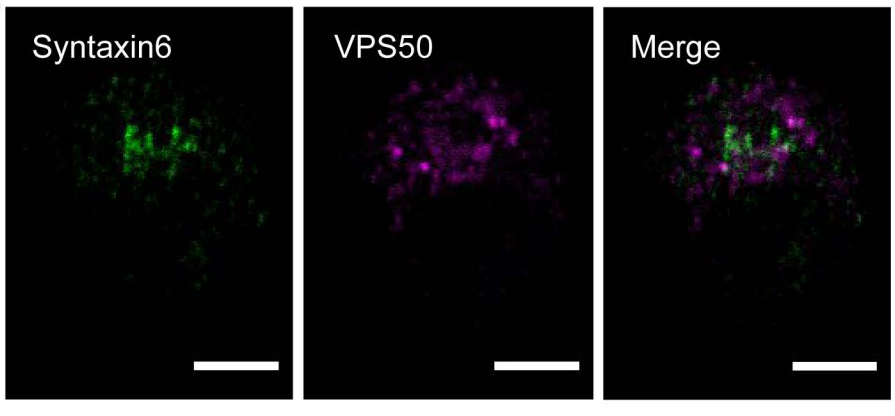

E